5 Techniques for prediction of subsidence, by Germán Figueroa Vega, Soki Yamamoto, and Working Group (Section 5.3.6 by Donald C. Helm)

It is very important to predict the amount of subsidence and to estimate the subsidence rate in the near future. There are many methods for predicting the amount of land subsidence due to the overdraft of fluids from aquifers. Some methods are simple and others are complex. It is preferable to use several methods whenever possible and to reach a conclusion based on the overall judgment.

Both adequate and accurate data are required to obtain useful results, although these depend on the purpose, time length of the forecast, and cost. The methods used may be classified into the following categories: (1) Empirical methods; (2) semi-theoretical approach; (3) theoretical approach.

5.1 EMPIRICAL METHODS

This is the method of extrapolating available data to derive the future trend. It is a time series model. The amount of subsidence, the amount of compaction, and sometimes tidal height near the sea coast, are available to plot against time. In this method, the amount of subsidence is considered a function of time, ignoring causality of land subsidence.

5.1.1 Extrapolation of data by naked eye

No explanation of this procedure is needed except that a smooth curve with a natural trend should be obtained.

5.1.2 Application of some suitable curve: Nonlinear extrapolation

1. Fitting of quadratic function (Figure 5.1):
   The following function is used and the least squares method is applied:

   $s = ax^2 + bx + c$, or $s = ax + b$, (5.1)

   where
   s = subsidence amount,
   x = time, and
   a, b, and c are constants.

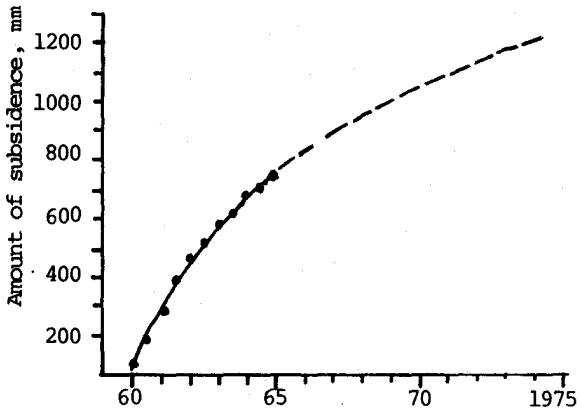

Figure 5.1 Fitting of quadratic curve (bench mark no. 2179, Niigata).

2. Fitting of exponential or logarithmic function (Figures 5.2 and 5.3):
   The following function is applied and the least squares method is used:

   $s = ax^b$, $\log s = \log a + b \log x$, or(5.2)

   $s = ae^{bx}$,

   where
   s = amount of subsidence,
   x = time, and
   a and b are constants.

Many data correlating land subsidence and water level have been published. Figures 5.4 through 5.7 are four examples of such correlations.

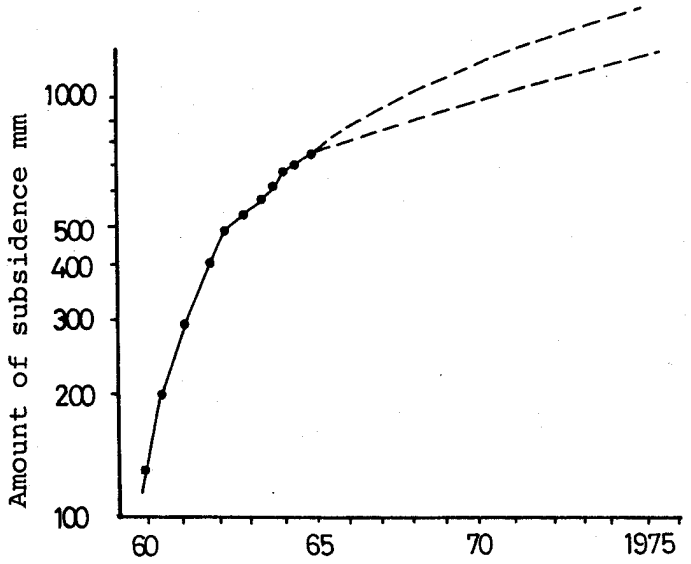

Figure 5.2 Fitting of exponential curve (bench mark no. 2179, Niigata)

.

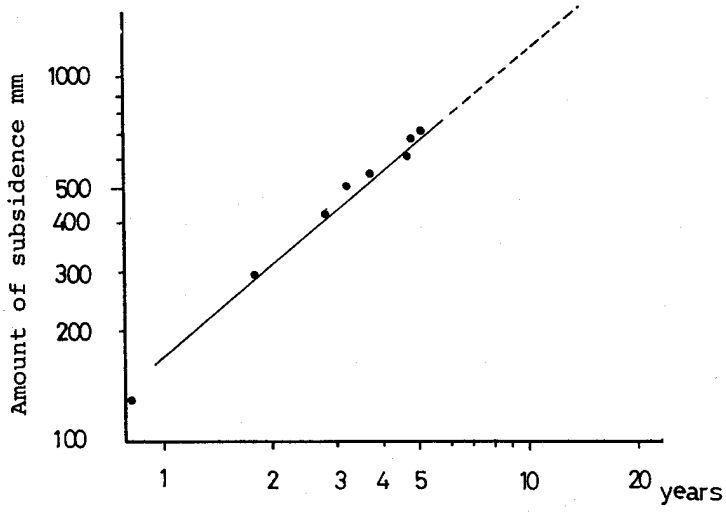

Figure 5.3 Log-log relation between subsidence and years.

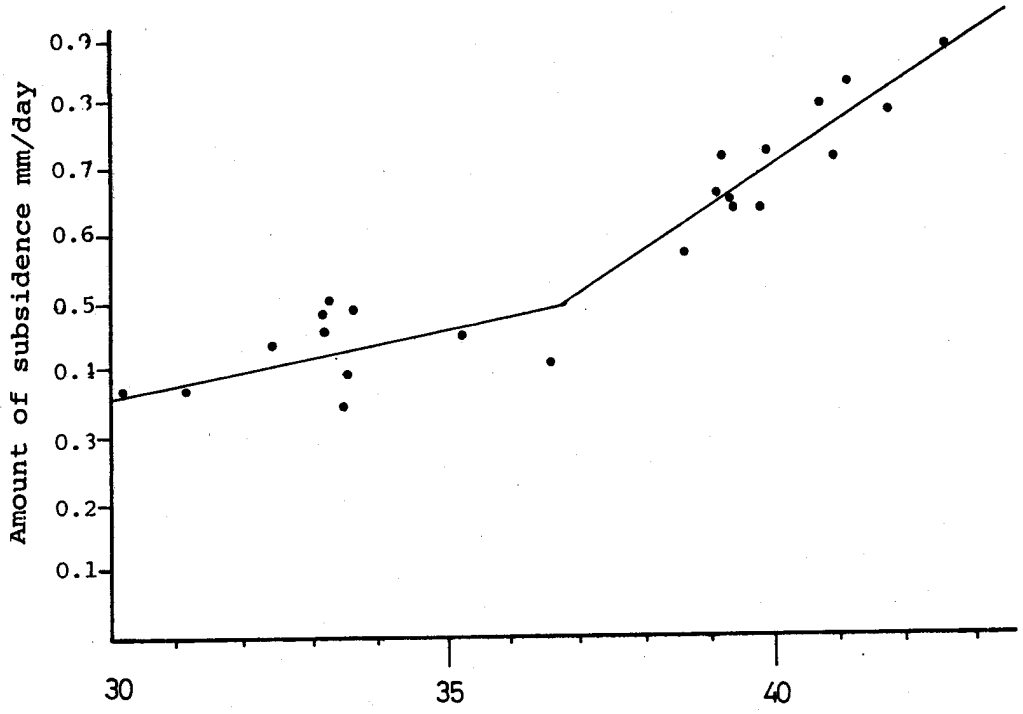

Figure 5.4 Correlation of land subsidence and water level in well 610 metres deep, Tokyo, Japan.

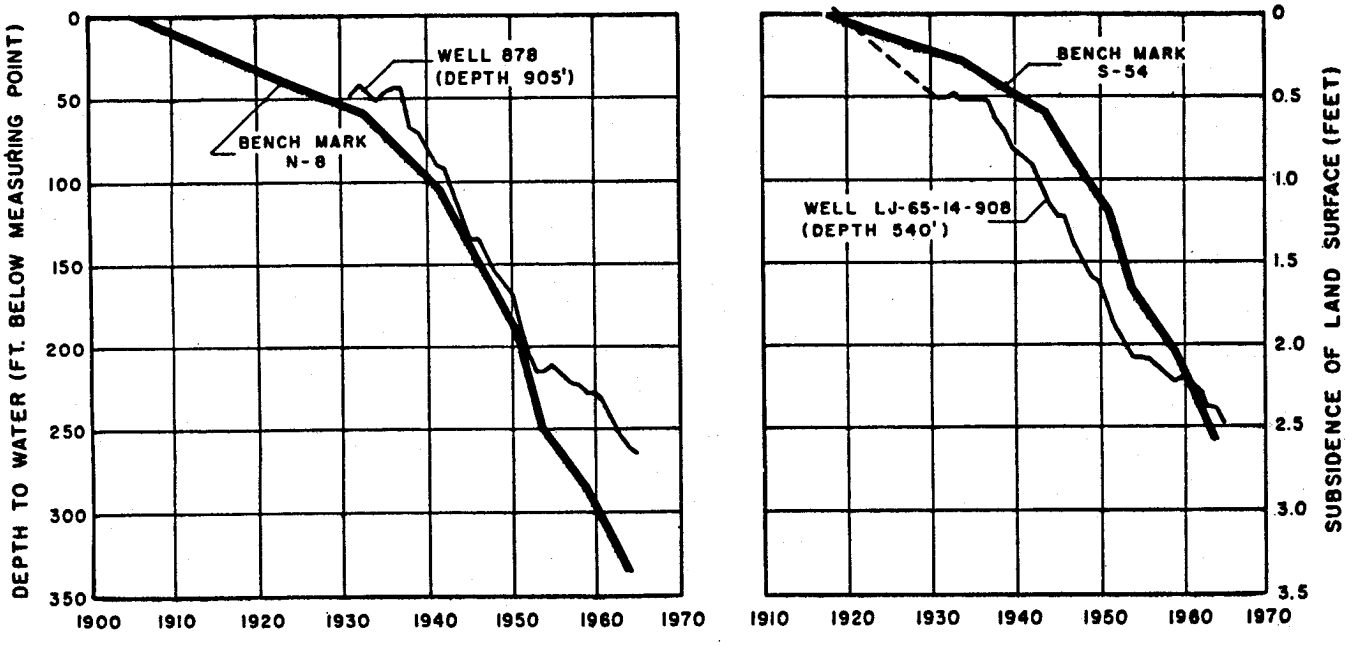

Figure 5.5 The relation between water-level declines and land-surface subsidence in the Houston area, Texas (Gabrysch, 1969).

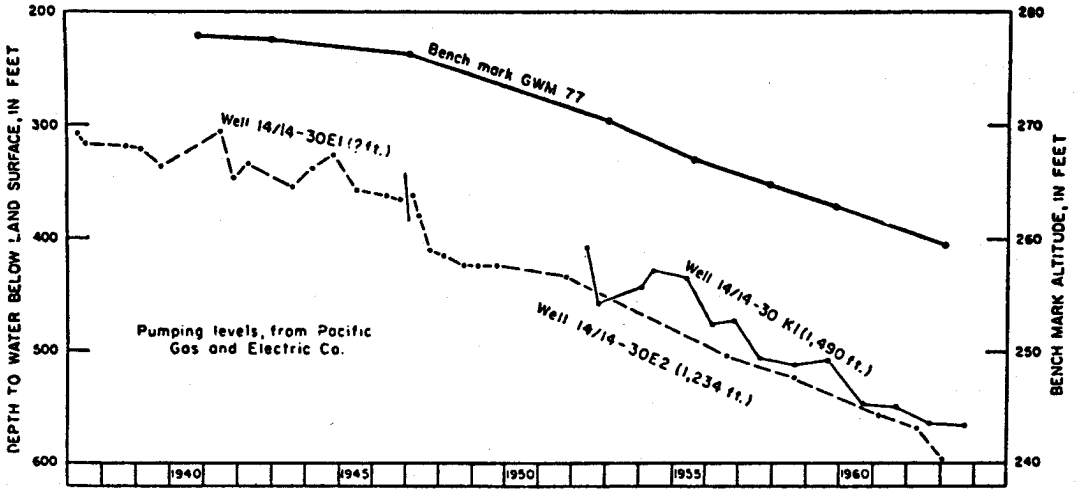

Figure 5.6 Correlation between subsidence and change in artesian head near center of subsidence west of Fresno, California (Lofgren, 1969).

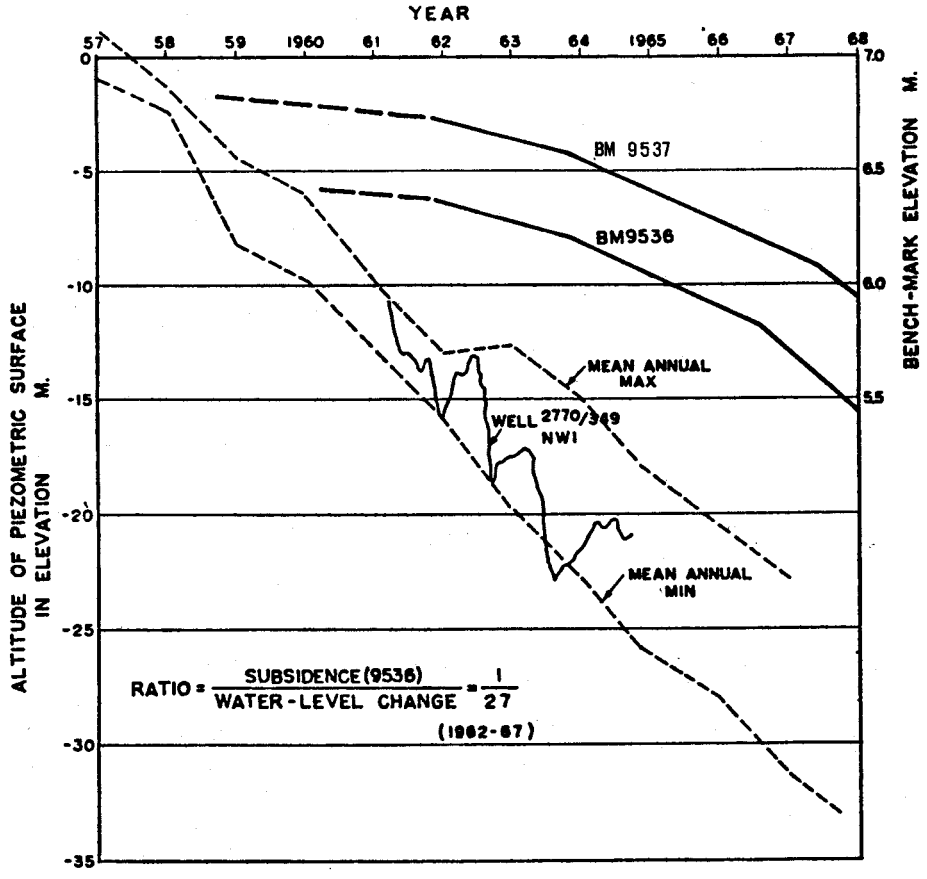

Figure 5.7 Change in altitude at BM9536, -37 and change in artesian head in nearby wells (Hwang and Wu, 1969).

5.2 SEMI-THEORETICAL APPROACH

This method utilizes the relation between subsidence and related phenomena. Although the relation is not strictly theoretical but rather an apparent one, still it can be used to estimate future trend.

5.2.1 Wadachi's (1939) model

Wadachi (1940) pointed out that the rate of subsidence, not the amount of subsidence itself, is proportional to the water-level change (Figure 5.8) and proposed the following equation:

$$\frac{dH}{dt} = k(p_0 - p) \tag{5.3}$$

where

$\frac{dH}{dt}$ = of subsidence,
p_0 = reference water level,
p = water level, and
k = a constant

This suggests that there exists a reference water level. That is to say, if the water level p recovers to the reference water level p_0, no subsidence occurs. But according to Yamaguchi's recent study (1969) there is no such reference water level. In place of Wadachi's equation, he proposed the following one:

$$\frac{ds}{dt} = ks_c\left\{(p_0 - p)t - \frac{dp}{dt}\right\}\exp\{-k(p_0 - p)t\}, \tag{5.4}$$

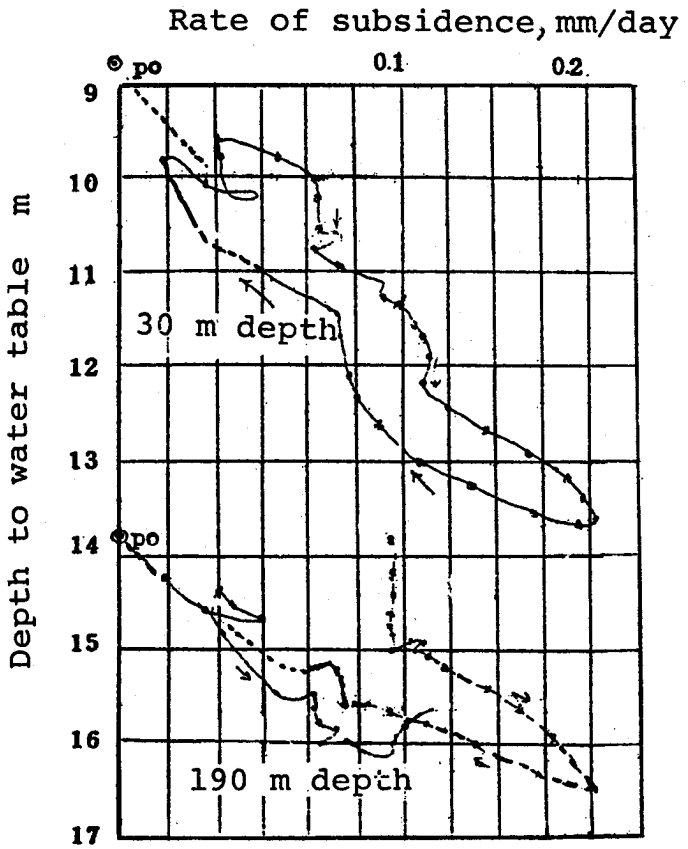

Figure 5.8 Relation between water level and rate of subsidence.

where

$\frac{ds}{dt}$ = rate of subsidence,
s_c = final subsidence amount,
P_0 = initial water level,
p = water level,
k = constant, and
t = time.

On solving this equation, the quantities

$$Y = \log\left[\frac{ds}{dt} \Big/ \left\{(p_0 - p)t - \frac{dp}{dt}\right\}\right] \text{ and } x = (p_0 - p)$$

are plotted on the respective axes as in Figures 5.9a and 5.9b and s_c can be obtained.

5.2.2 Ratio of subsidence volume to liquid withdrawal

According to Yamamoto (personal communication), the relation between liquid production and subsidence in the Niigata gas field (case history 9.7) has been expressed by the following equations, with fair results:

$$s = aQ + b, \text{ or } s = a\sqrt{Q} + b, \tag{5.5}$$

where
s = subsidence,
Q = amount of liquid production, and
a and b are constants.

Castle, Yerkes, and Riley (1969) stated that direct comparisons between the various measures of liquid production and subsidence in six oil fields showed a close relation. Correlation between production and subsidence has varied approximately linearly with net production (Figure 5.10).

The following relation has also been established but not yet published (Yamamoto, personal communication):

$$s = C/m_V \tag{5.6}$$

where
s = subsidence,
m_V = coefficient of volume compressibility, and
C = $\Delta H/\Delta Q$, where ΔH and ΔQ are the change of bench-mark elevation and the amount of production per unit area, respectively.

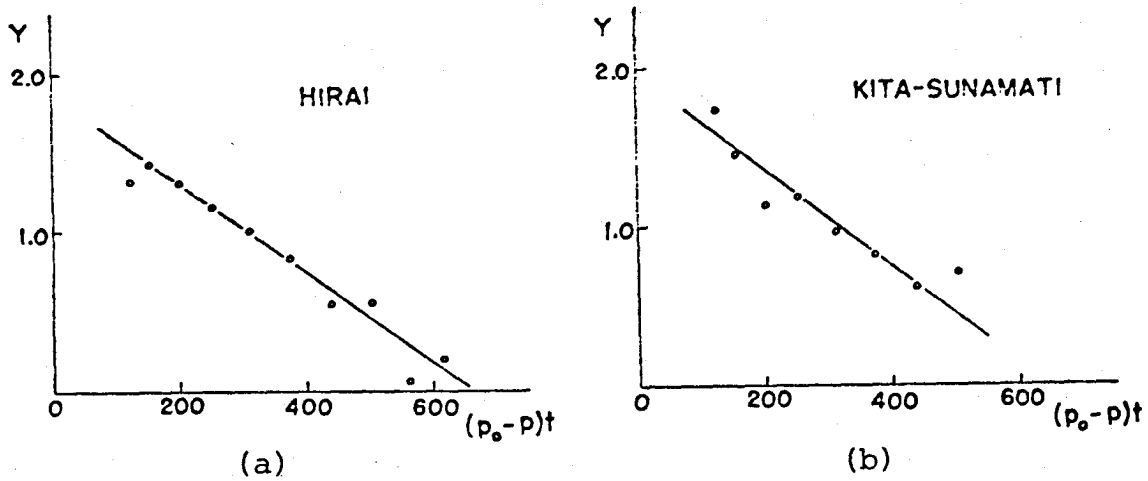

Figure 5.9 Relation between Y and $(p_0 - p)t$.

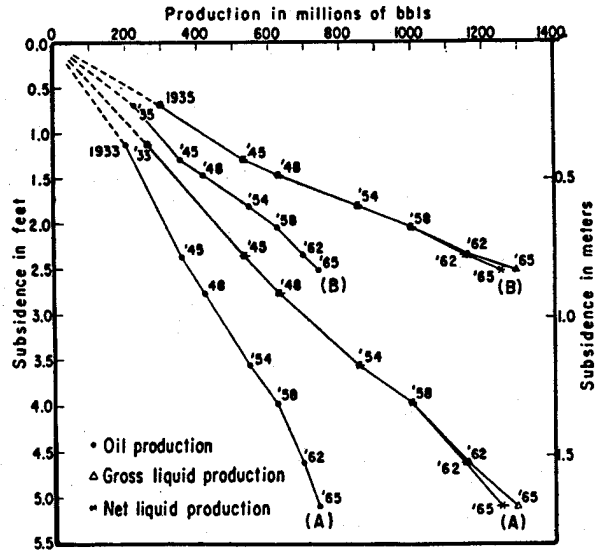

Figure 5.10 Cumulative oil, gross-liquid, and net-liquid production from the Huntington Beach oil field plotted against subsidence at bench marks located (A) near the center of subsidence and (B) midway up the southeast limb of the subsidence bowl. Prepared from production statistics of the California Division of Oil and Gas and elevation data of the U.S. Coast and Geodetic Survey and the Orange County Office of County Surveyor and Road Commissioner. Easily related elevation measurements have been available only since 1933; estimates of subsidence since 1920 shown by dashed lines (Castle, Yerkes, and Riley, 1969).

In one region in Japan, the change of the computed leakage rate, L, plotted against the measured volumetric land-subsidence rate, V_S, showed a close correlation (Figure 5.11).

On the Shiroishi Plain, Kyushu, Japan, Shibasaki et al (1969) proposed the following simple relationship for the data in the three-year period 1963 to 1966:

$$V_S = 0.27\ L + 0.25, \tag{5.7}$$

where each unit is expressed in $10^6 m^3$/mo (cubic metres per month) (Figure 5.12).

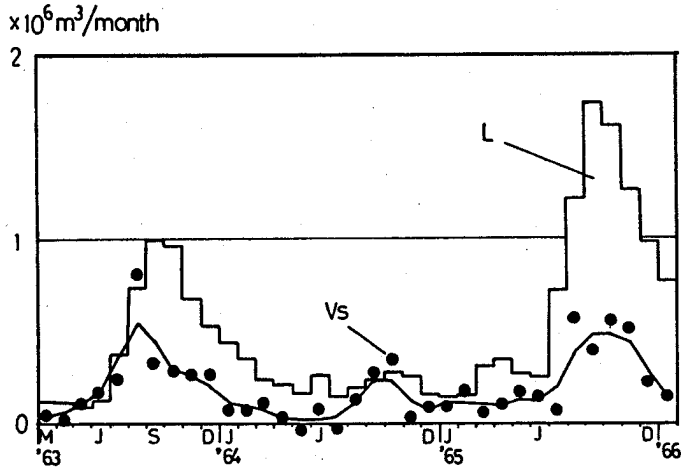

Figure 5.11 Changes of leakage rate, L, and volumetric land subsidence rate, V_S, both in m^3/month, over Shiroishi basin (Shibasaki, Kamata, and Shindo, 1960).

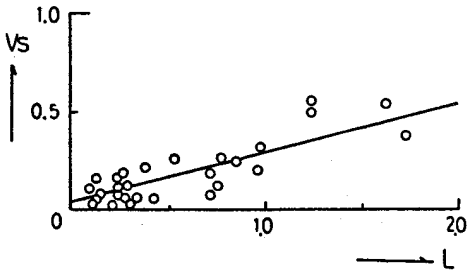

Figure 5.12 Simple relationship between leakage rate and volumetric subsidence rate over Shiroshi basin (Shibasaki, et al., 1969).

Although Castle, Yerkes, and Riley (1969) found that subsidence in six oil fields varied approximately linearly with net liquid production, the correlation between reservoir-pressure decline and subsidence was poor. Their explanation for this is as follows:

> "The general theory advanced in explanation of reservoir compaction and resultant oil-field subsidence (Gilluly and Grant, 1949) is, in its broad outlines, beyond challenge. Thus Terzaghi's principle, which relates increased effective stress directly to fluid pressure decline, probably is validly applied to the multifluid-phase system. Yet in seeming opposition to this generalization, measured reservoir pressure decline within the Vickers zone was disproportionately high with respect to surface subsidence during the early production years (Figure 2a and d); a similar situation is believed to have prevailed in the Wilmington field (City of Long Beach, 1967, unpublished data). Whatever the relationship, then, between measured reservoir pressure decline and compaction, the two are certainly not directly proportional.
> "The most likely explanation for the poor correlation between reservoir-pressure decline and subsidence (or compaction) is that pressure decline as measured at individual producing wells is generally non-representative of the average or systemic decline over the field as a whole. Thus in examining this problem in the Wilmington field, Miller and Somerton (1955, p. 70) observed that 'reductions in average pressure in the reservoir are virtually impossible to determine with a satisfactory degree of accuracy.' This deduction, coupled with the observed linearity between net-liquid production and subsidence, suggests that the liquid production may constitute a better index of average reservoir-pressure decline than that obtained through down-hole measurements."

Figures 5.13, 5.14, and 5.15 present additional examples illustrating the relation between fluid withdrawal and subsidence. Figure 5.13 shows the relation between land subsidence in mm/year and annual discharge in 106m3/year on the Shiroishi Plain in Japan (From Kumai, et al., 1969). Figure 5.14 illustrates the stress-strain relation obtained by plotting discharge in $10^3 m^3$/month against land subsidence in mm/month in Osaka, Japan, for the five years 1954-1958. Figure 5.15 shows the consistent relationship between the cumulative volumes of subsidence and ground-water pumpage in the Los Banos-Kettleman City area, California, from 1926 to 1968. The volume of subsidence was equal to one-third the volume of pumpage consistently through the 42-year period.

5.2.3 Ratio of subsidence to head decline

The subsidence/head-decline ratio is the ratio between land subsidence and the head decline in the coarse-grained permeable beds of the compacting aquifer system, for a common time interval. It represents the change in thickness per unit change in effective stress ($\Delta b/\Delta p'$). This ratio is useful for predicting a lower limit for the magnitude of subsidence in response to a step increase in virgin stress (stress exceeding past maximum). If pore pressures in the compacting aquitards reach equilibrium with those in adjacent aquifers, then compaction stops and the subsidence/head-decline ratio is a true measure of the virgin compressibility of the system. Until or unless equilibrium of pore pressures is attained, the ratio of subsidence to head decline is a transient value.

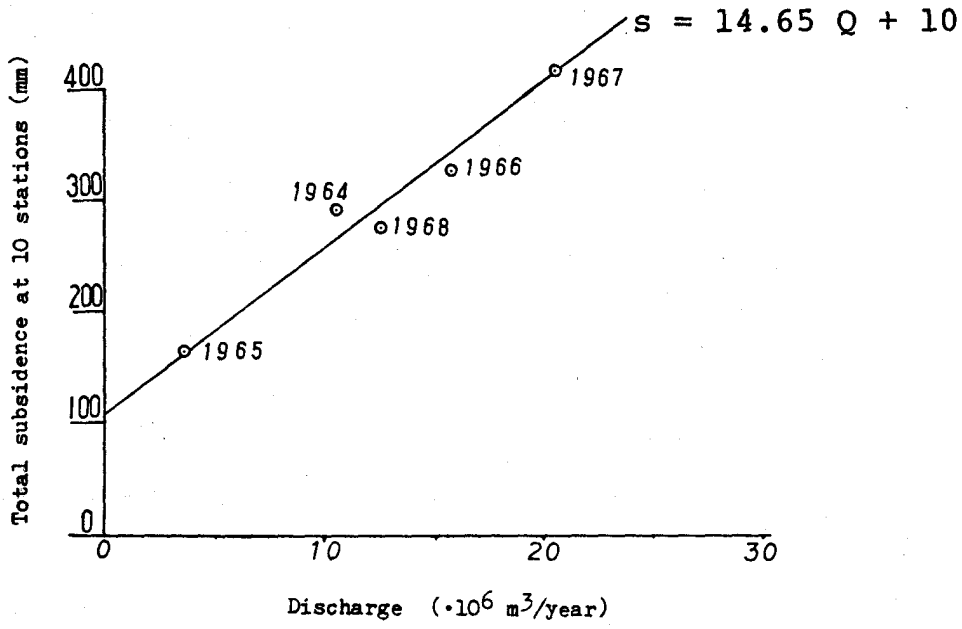

Figure 5.13 Simple relationship between annual land subsidence and corresponding discharge (Kumai, et al., 1969).

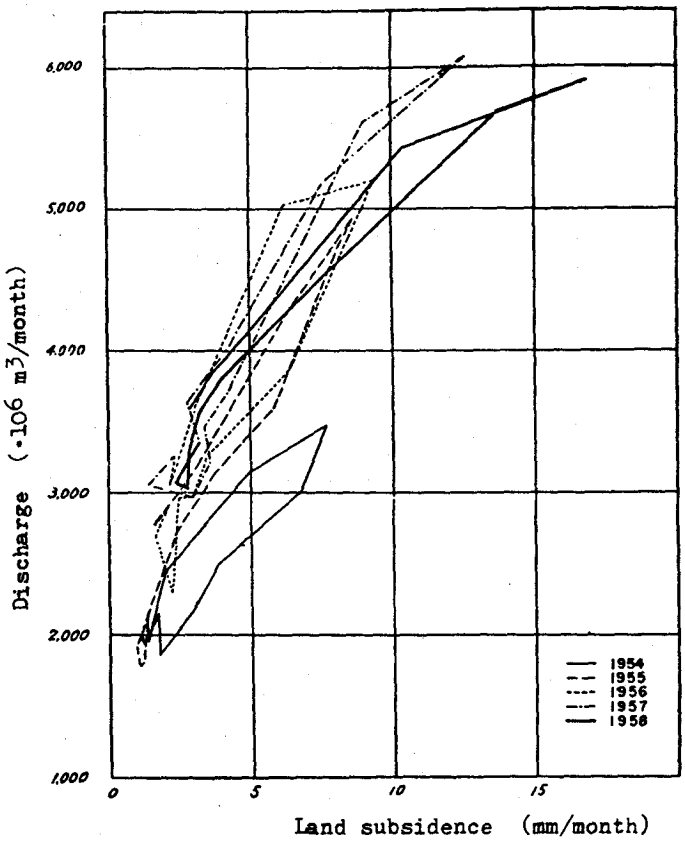

Figure 5.14 Correlation between subsidence and discharge of ground water (Editorial Committee for Land Subsidence in Osaka, 1969).

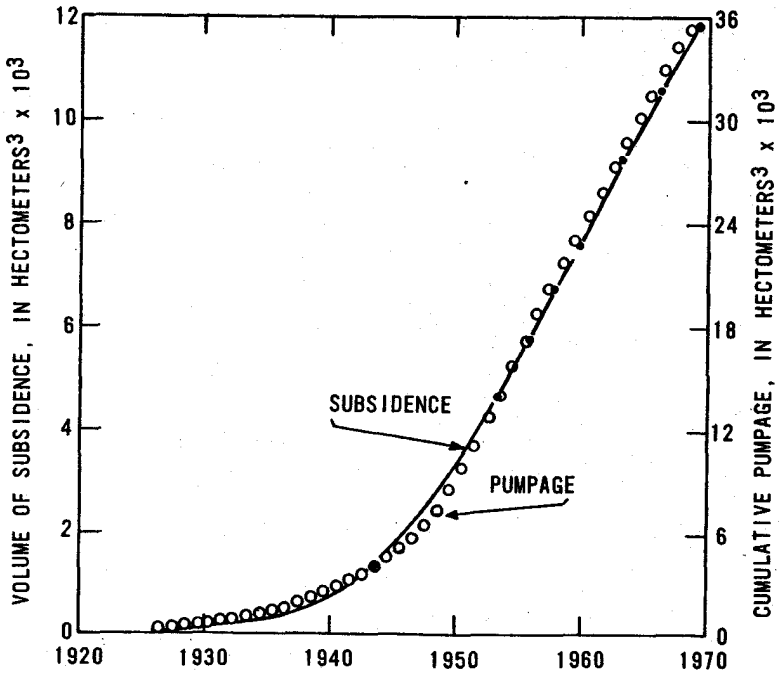

Figure 5.15 Cumulative volumes of subsidence and pumpage, Los Banos-Kettleman City area, California. Points on subsidence curve indicate times of leveling control (from Poland, et al., 1975).

Subsidence/head-decline ratios can be derived at a point if the water-level change for the compacting system and the periodic surveys of the elevation of a nearby bench mark are available for a common time period. For example, Figure 5.5 illustrates the subsidence and head-decline records for a pair of bench marks and nearby wells in Houston, Texas. At plotting scales of 1 (subsidence) to 100 (water level), the plots are roughly coincident. The indicated subsidence/ head-decline ratio is approximately 1/100.

Figure 5.6 is another example of close correlation between subsidence and head decline. The intensive pumping of ground water for more than two decades caused an artesian-head decline of about 300 ft (90m), producing a subsidence of about 18 ft (5.5 m). The indicated subsidence/ head-decline ratio is 1/16 (Lofgren, 1969). Although the ordinate scales in figures 5.5 and 5.6 are in feet, the ratio is dimensionless and hence would be identical in the metric system.

From the subsidence and head-decline record for Figure 5.7, Hwang and Wu (1969) derived a subsidence/head-decline ratio of 1/27 for the period 1962-67. Note, however, that although the mean annual minimum water-level trend is approximately a straight line, the rate of subsidence accelerated sharply in 1967. Hence, a ratio derived from the subsidence rate and water-level change in 1967 would be much larger, roughly about 1/12.

For all three of the examples discussed (Figures 5.5-5.7) it should be emphasized that the ratios are reliable only if the water levels are representative of the average artesian head in the aquifers (coarse-grained beds) of the compacting system.

If maps of subsidence and head decline are available for a common period of time during which both subsidence and head decline continued without interruption, the ratio of subsidence to head decline can be plotted on a map as lines of equal ratio. Figure 5.16 is such a ratio map, plotted from maps showing subsidence and head decline from 1943 to 1959 in an area of 4000 km^2 on the west side of the San Joaquin Valley, California (after Bull and Poland, 1975, Figure 32). The ratios on this map range from 0.08 to 0.01, indicating that the head decline required to produce 1 m of subsidence has ranged from 12 to 100 m, depending on the location. In addition to their use in prediction, the ratios in Figure 5.16 represent a minimum value of the storage coefficient component for virgin compaction of the aquifer-system skeleton.

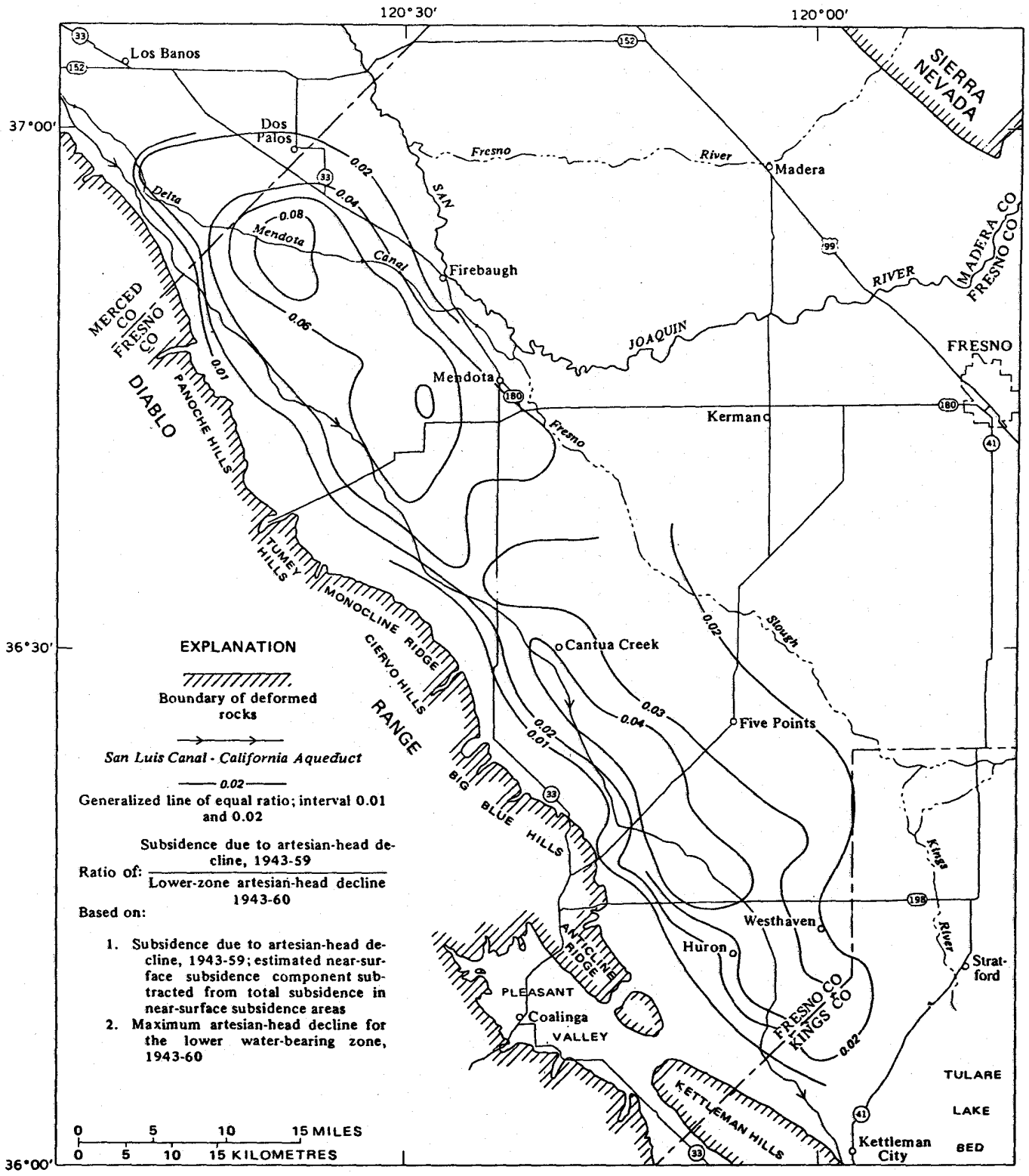

Figure 5.16 Ratio of subsidence to head decline, west side of San Joaquin Valley, California, 1943-59 (Bull and Poland, 1975, Figure 32).

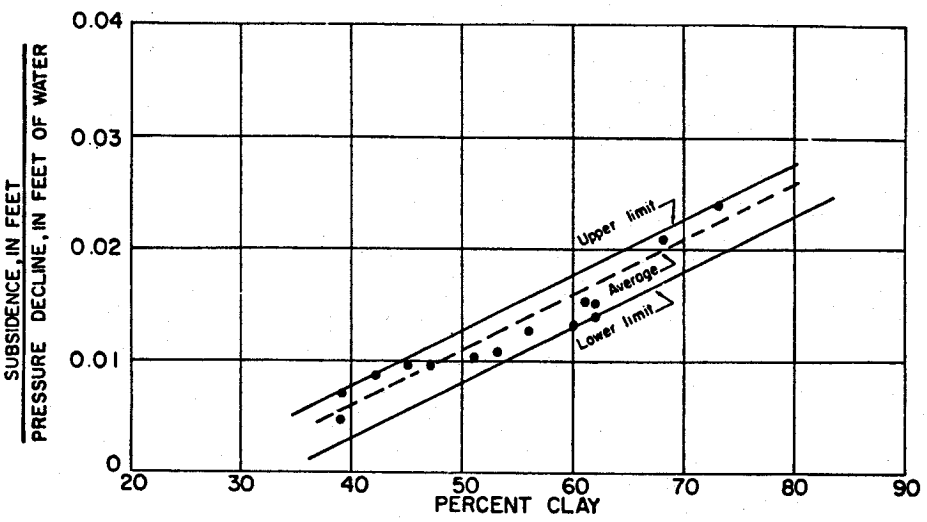

Figure 5.17 Relation between per cent clay and subsidence due to pressure decline (Gabrysch, 1969).

5.2.4 Clay content-subsidence relation

Figure 5.17 shows the general relationship in the Houston-Galveston area, Texas, between the percentage of clay beds and the subsidence head-decline ratio. According to Gabrysch (1969), the percentage of clay beds was determined from interpretation of electrical logs; the pressure-head decline was determined from measured water levels in wells; and subsidence values were taken from changes in nearby bench-mark elevations.

5.3 THEORETICAL APPROACH

5.3.1 General remarks

Regional subsidence due to ground-water extraction is a complex phenomenon which may be roughly "felt" in an intuitive fashion very difficult to explain quantitatively, due to the complexities of the materials involved.

Basically, the extraction of ground water reduces the interstitial water pressure (neutral pressure) which, according to the well-known "effective-pressure principle" of Terzaghi, means a transference of load to the soil skeleton (effective pressure) and its subsequent volume reduction (i.e., surface subsidence).

From a qualitative standpoint there is no "mystery" at all. However, in trying to explain the phenomenon both qualitatively and quantitatively, a series of unsuspected problems arise originating mainly from the elusive mechanical properties of soils.

Soils are complex multiple-phase systems constituted by solids, liquids, gases, and other substances like organic matter, ions, etc., which form, from a mechanical standpoint, a highly hyperstatic system whose properties must be inferred, at best, through statistical averages or "representative" tests.

As a result, soils incorporate into their mechanical properties all the behavioral aspects of their components, i.e. elasticity and plasticity of solids; viscosity of liquids; compressibility of gases; decay properties of organic matter; attraction and repulsion of ionic charges, etc., in a much more involved fashion.

This type of material has non-linear elastic, plastic, and viscous properties whose mechanical parameters are anisotropic and are history-, stress-, and time-dependent.

Such material is very difficult--if not impossible--to handle in any kind of a theoretical model of subsidence and this explains why the different approaches described in the scientific literature for that purpose, resort to many simplifications and idealizations in order to obtain some kind of a model that allows a more or less correct interpretation of past events, prediction of future ones, and decisions to be made about them. The questions are: What to simplify? How to idealize soils?

Unfortunately, there is no general rule, because the dominant feature in one case may be negligible in another and therefore, judgment and expertise must be exercised for best results. As general information, the more common simplifications regarding soil properties are listed here:

1. No organic matter present;
2. Only two phases present (solid-liquid);
3. No viscous properties;
4. No plastic properties;
5. Newtonian behavior of liquid phase;
6. No anisotropy;
7. Linear elastic properties of soil structure;
B. Constant parameters or, at least, one set for virgin compression and another for expansion and recompression.

Additionally, other simplifications regarding the system of aquifers and aquitards may be introduced, such as

9. Horizontal strata;
10. Horizontal flow in aquifers and vertical flow in aquitards;
11. Subsidence due mainly to aquitard consolidation;
12. No free surface of flow in the aquifers.

and so on.

As might be expected, the larger the number of simplifications made, the more restricted the nature of the resultant model and the more specific its applicability.

However, it should be remembered that, in practice, simplifications must be made according to the nature and volume of the available information and that the best way of modeling a given case may be to begin with the simpler models first, advancing later to the more involved ones, up to the highest level justified by the existing data.

In the remainder of this chapter an insight will be given on the details of several types of subsidence models (Figueroa Vega, 1973, 1977).

5.3.2 Compressibility relationships and total potential subsidence

The traditional laboratory test employed to disclose the compressibility relationships of soils is the consolidation test (odometer test) developed by Karl Terzaghi. The test is discussed in Chapter 4.

In this test, soils exhibit a more or less linear relationship between e (void ratio) and log p'/p_0', effective intergranular pressure) of the type

$$e = e_0 - C_C \log \frac{p'}{p_0'}, \tag{5.8}$$

(a slightly modified form of equation 4.14 shown in Chapter 4), where Cc is the "compression index" and eo and pol are initial reference values. This relationship is valid for increasing values greater than the maximum intergranular pressure the soil has supported in the past (pol, preconsolidation pressure). For discharge or recharge at pressures lower than the preconsolidation pressure (i.e.: within preconsolidation range) the relationship is similar, with a lower Cc value (Cc), which means that only part of the total deformation of a soil is recoverable and also that the compressibility parameters of a soil are history dependent.

In the soil mechanics field, it is customary to define the "coefficient of volume compressibility," m_V, as

$$m_V = \frac{\frac{de}{dp'}}{1 + e_0} = \frac{a_V}{1 + e_0}, \tag{5.9}$$

where a_V stands for the coefficient of compressibility, such that, within a small increment of pressure, the total settlement of a column of soil of thickness, H_0, may be computed as

$$\Delta H = m_V \, \Delta p' H_0. \tag{5.10}$$

As may be noted in equation (5.9), m_v, is stress dependent and therefore its value must be estimated for the proper e_0 and $\Delta p'$ values. Otherwise, equation (5-10) may lead to serious errors.

Equation (5.10) may be applied directly--as in the soil mechanics field--as a first approximation, whenever the strata thickness sequence is known (H_{01}, H_{02}, ..., H_{0i}) as well as the corresponding neutral pressure reductions due to water extraction (taken initially as the effective pressure increments) and their estimated coefficients of volume compressibility (m_{v1}, m_{v2},....,m_{vi}). The total subsidence in this case would be approximately

$$\overline{\Delta H} \approx \sum_{1}^{i} m_{vi} \Delta P_i' H_{oi} . \tag{5.11}$$

When all the involved strata remain saturated and the total relative shortening of the column is small, the foregoing calculations may be accepted as sufficiently good for practical purposes. In other cases, they must be taken only as giving approximate values and subsequent calculations must be made utilizing these values to estimate the total initial and final column loads at each level, the initial and final effective pressures (vertical pressure due to total load) and applying again equation (5.11) and repeating the process iteratively, until final results take account properly of both effects.

5.3.3 Differential equations of ground-water flow in an aquifer-aquitard system

Steady laminar flow of interstitial water within any portion of saturated soil obeys two basic laws--the mass conservation law:

$$\mathrm{div}(\gamma \bar{v}) = 0 , \tag{5.12}$$

where "div" stands for the divergence operator, "γ" for density of water, "v" for flow velocity vector, and Darcy's Law:

$$v = -K \ \mathrm{grad}\ h, \tag{5.13}$$

where K is the hydraulic conductivity of the soil and "h" the hydraulic head.

Combining these laws into a single equation and neglecting the variability of γ and K gives

$$\nabla^2 h = \frac{\partial^2 h}{\partial x^2} + \frac{\partial^2 h}{\partial y^2} + \frac{\partial^2 h}{\partial z^2} = 0 , \tag{5.14}$$

the well-known Laplace equation. Therefore, h must be an harmonic variable satisfying the existing boundary conditions.

Equation (5.12) simply states that the mass of water within the portion of saturated soil remains constant. When the flow is unsteady, this does not hold anymore and some water is stored in or extracted from a specified elemental volume of soil and equation (5.14) must be modified accordingly, resulting in

$$K\nabla^2 h = S_s \frac{\partial h}{\partial t} , \tag{5.15}$$

where "S_S" is the specific storage and a linear compressibility relationship is assumed both for water and soil structureo.

In a homogeneous horizontal aquifer of constant thickness "b" with horizontal flow, equation (5.15) reduces to

$$\frac{\partial^2 h}{\partial x^2} + \frac{\partial^2 h}{\partial y^2} = \frac{S_s}{K}\frac{\partial h}{\partial t} = \frac{S}{T}\frac{\partial h}{\partial t} = \frac{1}{v}\frac{\partial h}{\partial t} , \tag{5.16}$$

where

$$S = bS_S;\ T = bK;\ \text{and}\ v = \frac{T}{S} \tag{5.17}$$

are the storage coefficient, transmissivity and hydraulic diffusivity respectively. In a compressible aquitard with vertical flow, equation (5.15) reduces simply to

$$\frac{\partial^2 h}{\partial z^2} = \frac{1}{\nu}\frac{\partial h}{\partial t}\,. \tag{5.18}$$

These equations may also be written in terms of "s" (drawdown) instead of "h" (hydraulic head).

Equation (5.16) is the classical aquifer differential equation due to Theis (Theis, 1935) and equation (5.18) is the classical consolidation equation due to Terzaghi (Terzaghi, 1923). Both equations must be solved subject to their proper initial and boundary conditions.

In a system with aquifer(s) and aquitard(s), the mathematical problem to solve is made up of one equation of the type (5.16) for each aquifer including some additional terms to take account of vertical inflows or outflows, if any, and one equation of the type (5-18) for each aquitard, plus the adequate initial and boundary conditions and additional conditions stating equality of hydraulic heads in any plane of contact of any two of the existing aquifer(s) and aquitard(s). This is referred to as a "quasi three-dimensional model." The final result is a complex coupled system which may be solved with the help of numerical methods (finite differences or finite elements). The assumption of vertical flow in aquitards and horizontal flow in aquifers is only justified when the permeability of the latter is much higher than that of the former (say tenfold or more). Otherwise, it is necessary to resort to a truly three dimensional model, where all the second order partial derivatives are kept for all the strata.

The solution of the coupled system implies advancing numerically and simultaneously the solution for all the involved strata through each time increment, and this may represent a large number of calculations which might eventually overflow the working capability of the available computer. Models of this kind have been developed and published elsewhere (Carrillo, 1950; Gambolati, 1972).

An interesting alternative solution, for quasi three dimensional models, as applied to the Mexico City case (Figueroa V, 1973), is to depart from a coupled system to reduce the problem's complexity via integrodifferential equations. This will be outlined in the next section.

5.3.4 Uncoupling the system and solving a simpler problem

For a system made up of one aquifer underlain and overlain by consolidating aquitards, several mathematical formulations are possible in accordance with the upper and lower boundary conditions type (constant head or null flow). In any case, the mathematical formulation is made up, in terms of drawdowns, as explained before, by one equation of the type (5.16), including in its left side two terms of the form

$$\mp\frac{K_i}{T}\frac{\partial}{\partial z}s_i(x, y, 0, t) \tag{5.19}$$

to take account of vertical flow into the main aquifer, through the aquifer-aquitard common boundaries, plus two equations of the type (5.18) also in terms of drawdowns, plus the corresponding initial and boundary conditions.

For all the resulting cases of this system it has been shown (Herrera and Figueroa, 1969) that the problem was equivalent to

$$\frac{\partial^2 s}{\partial x^2} + \frac{\partial^2 s}{\partial y^2} + \int_0^t \frac{\partial}{\partial t}s(x, y, \beta)G(t-\beta)\partial\beta = \frac{1}{\nu}\frac{\partial s}{\partial t}\,, \tag{5.20}$$

where the convolution term includes the vertical inflows to the aquifer, and

$$G(t) = \frac{K_1}{T}\frac{\partial}{\partial z}A_1(0, t) - \frac{K_2}{T}\frac{\partial}{\partial z}A_2(0, t) \tag{5.21}$$

in which G(t) is the zero elevation at the aquifer-aquitard contacts and A_1 and A_2 the basic

solutions of classical consolidation theory corresponding to the particular boundary conditions present in each case. Additionally, in general

$$G(t) = -C - F(t) \tag{5.22}$$

where "C" is a constant depending on the system's parameters which incorporates the vertical inflows coming from the exterior boundaries of the system in the cases of constant head boundary conditions, and the function F (t) incorporates the vertical inflows released from aquitards by consolidation.

Equation (5.20) may be reduced to

$$\frac{\partial^2 s}{\partial x^2} + \frac{\partial^2 s}{\partial y^2} - C_s - \int_0^t \frac{\partial}{\partial \beta} s(x, y, \beta) \bullet F(t-\beta) \partial \beta = \frac{1}{\nu} \frac{\partial s}{\partial t} . \tag{5.23}$$

Furthermore, the integral term may be approximated by

$$\int_0^t \frac{\partial}{\partial \beta} s(x, y, \beta) \bullet F(t-\beta) \partial \beta = I \frac{\partial}{\partial t} s(x, y, t) \tag{5.24}$$

when $\partial s / (\partial \beta)$ has a slow variation, being

$$I = \int_0^\infty F(\beta) \partial \beta , \tag{5.25}$$

a constant. Under these conditions, the problem further reduces to

$$\frac{\partial^2 S_c}{\partial x^2} + \frac{\partial^2 S_c}{\partial y^2} = \frac{1}{\nu_c} \frac{\partial S_c}{\partial t} , \tag{5.26}$$

where

$$S_c = s e^{c \nu_c t} \tag{5.27}$$

and

$$\nu_c = \frac{\nu}{1 + I_\nu} . \tag{5.28}$$

This is the "correspondence principle" (Herrera and Figueroa, 1969). It means that the original coupled system is equivalent, under the already stated conditions, to an equivalent confined aquifer system.

For the case of a single aquifer and a single aquitard, the applicable expressions are

$$G(t) = -\frac{K_1}{T b_1} 1 + 2 \sum_{n=1}^{\infty} \exp - \frac{n^2 \pi^2 \nu_1}{b_1^2} t , \tag{5.29}$$

$$I = \frac{S_1}{3T}; C = \frac{K_1}{T b_i}; \nu_c = \frac{3T}{3S + S_1} \tag{5.30}$$

for the constant head external boundary condition and

$$G(t) = -\frac{2K_1}{Tb_1}\sum_{n=0}^{\infty}\exp\left(-\frac{\left(n+\frac{1}{2}\right)^2\pi^2\nu_1}{b_1^2}t\right), \tag{5.31}$$

$$I = \frac{S_1}{T};C = 0;\nu_c = \frac{T}{S+S_1}, \tag{5.32}$$

for the zero gradient external boundary condition. In all these formulas, the index 1 refers to the aquitard.

Both the integrodifferential equation and the correspondence principle have been applied to the Mexico City case, with some additional considerations which will be mentioned later, with reasonably good results. As a general comment, the applicability of the above-mentioned simplifications of the correspondence principle is much greater than it seems, for the following reasons.

Apparently, the correspondence principle would be applicable whenever $\partial s/\partial t$ "has a slow variation" as stated before. However in the extreme case of constant drawdown the right part of equation (5.24) equals zero for $t \neq 0$, which means that there is no consolidation except at $t = 0$, where the subsidence cause is concentrated. So, the former condition should read "has a slow variation everywhere."

It must be noted that equation (5.24) simply removes the lag-effects of the consolidation process and therefore it may work only if the drawdown is gradual. The more $\partial s/\partial t$ departs from a constant value the more the results depart from reality.

However, the consolidation process compensates this situation somehow, because while at any time increment, the subsidence increment includes some subsidence due to the preceding drawdowns, also part of the subsidence due to its own drawdown increment is transferred to future time increments. In any case, a short consolidation time may improve the results.

It is possible that an integration by parts of the memory term could lead to a better approximation, and this is a question which must be explored.

Another reason which supports the correspondence principle is the remarkably good correlation found between total drawdown and total subsidence.

According to the experience gained in the Mexico City case, from a practical standpoint there seems to be no strong reason to use equation (5.26) instead of equation (5.23) as there is not a big difference in computing time or computer memory requirements. So, its use seems to be more practical in non-computer modeling, as described in the next section.

In applying equation (5.23), some aspects must be considered:

1. Additional terms must be included to take into account infiltration or pumpage.
2. Compressibility parameters must distinguish between virgin compression and elastic recompression.
3. The storage coefficient in the main aquifer must be changed in those cells of the model where drawdowns are such that ground-water flow changes from confined to unconfined.
4. The aquifer compaction itself, if considered relatively important, may be added, computing it as an instant response to drawdown, thus taking care of point (b), above.

The procedures described herein may be incorporated in any of the existing types of ground-water models.

5.3.5 Simplified subsidence modeling

In some cases it may be desirable to have a fast estimate of the probable order of magnitude of subsidence versus time due to regional pumpage in some selected site(s) and this may be done through (1) estimating future drawdowns in the site(s) and (2) estimating future subsidence in the site(s).

The first part may be achieved by simple superposition of the Theis equation or by the application of the Influence Diagram (Figueroa Vega, 1971), together with the application of the aforementioned Correspondence Principle (equations 5.26, 5.27 and 5.28).

The superposition of the Theis equation needs no further comment. It may be advisable when the number of wells is not too large.

When there are many wells and their distribution is fairly uniform with an average pumpage of "q" units of volume per unit of time, it is much more practical to apply the influence diagram mentioned before, which is a diagram similar to that developed by Newmark (1942) in the soil mechanics field to integrate vertical stresses due to a distributed surcharge.

By means of it, drawdown "s" at the site and at time "t," due to a distributed pumpage of intensity "q" in any area is simply

$$s = \frac{qt}{S}(0.0025N_i + 0.001N_e), \tag{5.33}$$

where "S" is the storage coefficient and "N_i" and "N_e" are the internal and external "squares" covered by the pumping area drawn at a proper scale.

The application of equation (5.33) for several times makes it possible to plot estimated future drawdowns versus time.

The next step is to estimate the future subsidence, the time derivative of which is T (transmissibility) times the convolution term of the left side of equation (5.23), i.e.:

$$\frac{\partial h}{\partial t} = T\int_0^t \frac{\partial}{\partial \beta} s(x, y, \beta) \bullet F(t-\beta)\partial\beta \, . \tag{5.34}$$

This expression may be easily approximated by numerical methods with the help of a pocket programmable calculator and the total subsidence for each time is the area under the curve versus t.

Equation (5.34) takes only into account the consolidation of the clay strata. Compression of the aquifer may be included, as an instant response for each increment of time, using equation (5.11).

The former procedure, though simple and lacking precision, may be used as a basis for preliminary decision-making in many cases of regional subsidence due to ground-water extraction, while a more precise digital computer model is elaborated and validated.

5.3.6 Other types of subsidence models, by Donald C. Helm[2]

A variety of prediction techniques have been discussed--empirical, semi-theoretical, and theoretical. The empirical and semi-theoretical techniques require induced subsidence to have already begun. Empirical and semi-theoretical methods offer reasonable parameters that link subsidence to some other measurable phenomenon in the field. The theoretical techniques which have been discussed to this point require the results of laboratory tests in order to predict subsidence.

Two other techniques for subsidence prediction will now be discussed. This will be followed by a discussion of the role of the unpumped overburden. One technique, which uses a depth-porosity model, is too primitive to require induced subsidence to have already begun. This is its power; it can give a rough approximation of potential ultimate subsidence of an area where the local confined aquifer system has not yet been stressed. The second technique that will be discussed uses an aquitard drainage model. In contrast to the depth-porosity model, this second technique requires compressible beds to be stressed in the field. It is sufficiently sophisticated not to require laboratory tests on soil specimens. Neither the depth-porosity model nor the aquitard-drainage model requires laboratory tests; each uses its own independent field-based method for parameter evaluation. They are both useful techniques.

The parameter found by using the depth-porosity model is a generalized depth-dependent approximation for a coefficient of volume change, m_v, of equation 5.10 which corresponds to nonrecoverable specific storage, S'_{skv}, of equations 3.4 and 3.19. This parameter controls the ultimate response to stress of a specified bed. The parameters found by using the aquitard drainage model are site-specific average values of specific storage, S'_{skv}, and the vertical component of hydraulic conductivity, K'. These parameters control the time-delayed response to

---

[2] Work performed under auspices of the U.S. Department of Energy by the Lawrence Livermore National Laboratory under contract No. W-7405-ENG-48.

stress of compressible interbeds within a confined system. They appear directly in equation 3.2 and indirectly in equation 5.15.

5.3.6.1 Depth-porosity model

Porosity of sedimentary materials is known to decrease in general with depth (Figure 5.18). Based on empirical data for shale and mudstone, Athy (1930) and Magara (1978) suggest that a relation between porosity and depth can be found from an exponential expression

$$n + n_0 e^{-cz} \tag{5.35}$$

for conditions of compaction equilibrium where n is porosity at a specified depth z, n_0 is an extrapolation of n to land surface (z = 0), and c is an empirically determined constant. For Athy's data of shale porosities from Oklahoma, n_0 equals 0.48 and c equals 0.0014 when z is expressed in metres. Schatz, Kasameyer, and Cheney (1978) suggest using equation 5.35 for site-specific values for n_0 and c as a means of approximating S'_{skv} as a function of depth, z, for all compressible sedimentary material including shale, mudstone, sandstone, and clay. They tacitly argue that decreasing fluid pressure due to producing an artesian aquifer system has an

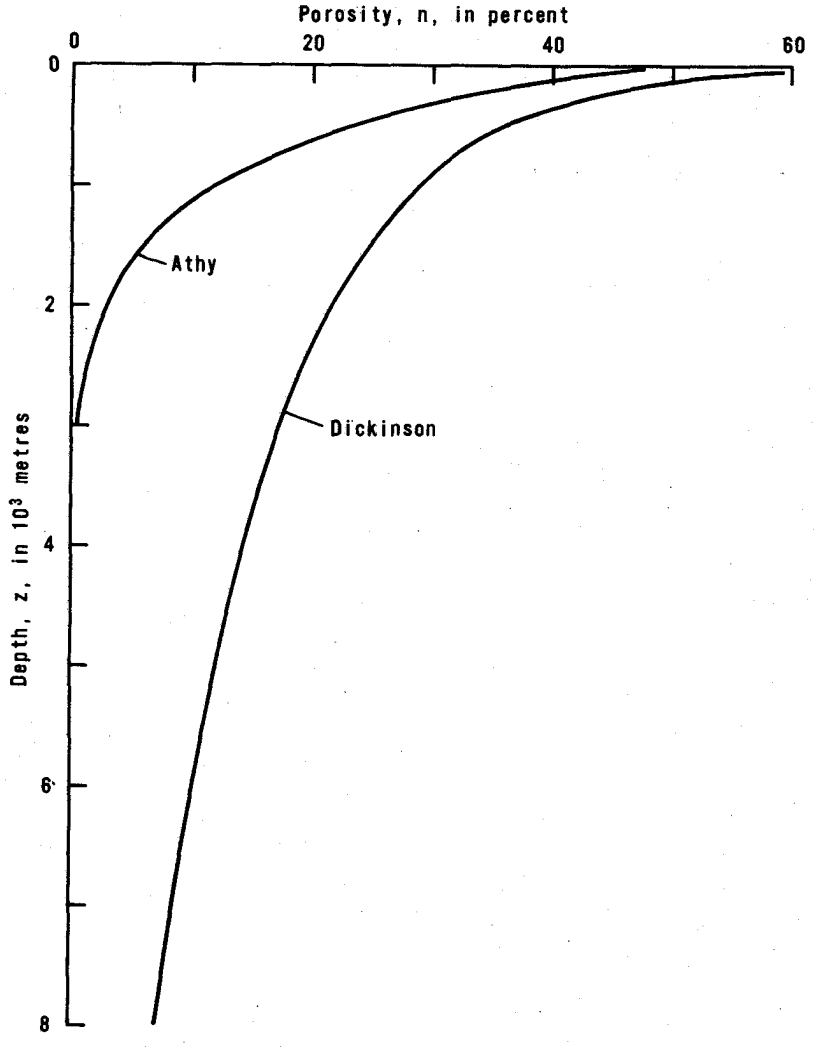

Figure 5.18 Two examples of decrease of porosity with depth.

equivalent effect on porosity that lowering the bed to a greater depth would have. Hence the curves in Figure 5.18 are treated by them to represent a type of ultimate stress/strain relation for equilibrium compaction.

Unfortunately, not all empirical depth-porosity curves follow an exponential relation as expressed by equation 5.35. A notable exception (Magara, 1978, p. 93) is Dickinson's (1953) data for shale porosities from the Gulf of Mexico coast. Helm (1980, unpublished manuscript) has found that Dickinson's shale porosities follow a logarithmic relation with depth, namely

$$\Delta n = -a\ \Delta \ln x, \tag{5.36}$$

$$n = n_{ref} - a\ \ln(z/z_{ref}), \tag{5.37}$$

where n_{ref} and z_{ref} are reference values for porosity and depth and a is an empirical constant. If a is interpreted as a type of compression index, equations 5.36 and 5.37 approximate the type of stress-strain relation one would anticipate from standard soil mechanics interpretation of laboratory consolidation data. For Dickinson's field data from the Gulf Coast, a equals 0.103 and n_{ref} is found to equal 0.05 for an arbitrary reference depth z_{ref} of 10^4 m.

It is now possible to get two depth-dependent theoretical values of S'_{skv} based on equations 5.35 and 5.37. Recalling equation 3.10, we can express how lithostatic effective stress, p', due to submerged weight of overlying material changes with depth, z, by the gradient

$$\frac{dp'}{dz} = (1-n)(G-1)\gamma_w = \frac{G-1}{1+e}\gamma_w . \tag{5.38}$$

According to the left-hand equality of equation 3.4 and equation 5.9, we write

$$S'_{skv} = -\frac{1}{1+e}\frac{de}{dp'}\gamma_w = -(1-n)\frac{de}{dp'}\gamma_w . \tag{5.39}$$

Equation 5.39 can be written

$$S'_{skv} = -(1-n)\frac{de}{dn}\frac{dn}{dz}\frac{dz}{dp'}\gamma_w = -\frac{\gamma_w}{1-n}\frac{dn}{dz}\frac{dz}{dp'}, \tag{5.40}$$

which, in accordance with equation 5.38, becomes

$$S'_{skv} = -\frac{1}{(1-n)^2(G-1)}\frac{dn}{dz} . \tag{5.41}$$

It now becomes necessary to determine dn/dz from Figure 5.18. For Athy's curve, equation 5.41 becomes

$$S'_{skv} = \frac{c}{(G-1)}\frac{n}{(1-n)^2}, \tag{5.42}$$

where we have used equation 5.35. For Dickinson's curve, however, equation 5.41 becomes

$$S'_{skv} = \frac{a}{(G-1)z(1-n)^2} \tag{5-43}$$

where we have used equation 5.37.

Figure 5.19 shows the relation of S'_{skv} and depth z in accordance with Athy's data (dashed line) and Dickinson's data (solid line). The dashed line in Figure 5.19 was found by substituting equation 5.35 into the right-hand side of equation 5.42 and assuming n_0 to equal 0.48 and c to equal 0.0014. The solid line in Figure 5.19 was similarly found by substituting equation 5.37 into the right-hand side of equation 5.43 and assuming n_{ref} to equal 0.05, Z_{ref} to equal 10^4 m, and a to equal 0.103.

The marks on Figure 5.19 indicate a selection of S'_{skv} values determined by other methods. The X's in the upper right-hand corner of Figure 5.19 represent values of S'_{skv} calculated from results (Marsal and Graue, 1969, Table 5, p. 190) of standard laboratory consolidation tests on soil samples near Mexico City. The symbols X_{SC}, X_T, and X_W represent values of S'_{skv} calculated from results of standard laboratory consolidation tests on soil samples taken respectively from the Santa Clara Valley, California (Poland, written communication, 1978), from near Seabrook,

Texas (Gabrysch and Bonnet, 1976, Table 3), and a composite of values from the Wilmington Oil Field, California (Allen and Mayuga, 1969). Subsidence is known to have occurred at all these sites. The circles represent values of S_{skv} determined from simulating observed compaction and expansion in California by means of a digital computer code. This computer simulation technique uses the aquitard-drainage model and is discussed in the next section.

It is evident from Figure 5.19 that within 1000 metres of land surface, Dickinson's curve gives a high, but reasonable, estimate of S'_{skv}. Helm (1980, unpublished manuscript) suggests the use of the solid curve in Figure 5.19 as a first approximation of S'_{skv}, For example, assume a confined aquifer has not been developed and hence no field-based compaction records are available. However, suppose one knows that an areally extensive confined aquifer system lies at a depth between roughly 100 and 300 metres. Within this 200-metre interval there is found to exist about 100 metres of fine-grained compressible interbeds. Hence the thickness of compressible beds, b', is about 100 m, the average depth is about 200 m, and in accordance with Dickinson's curve in Figure 5.19 we can estimate S'_{skv} to approximate $10^{-3}m^{-1}$. Using equation 3.4, we find

$$\Delta b'/\Delta h_a = S'_{skv}b' \cong 10^{-3} \times 10^{2} = 10^{-1}. \qquad (5.44)$$

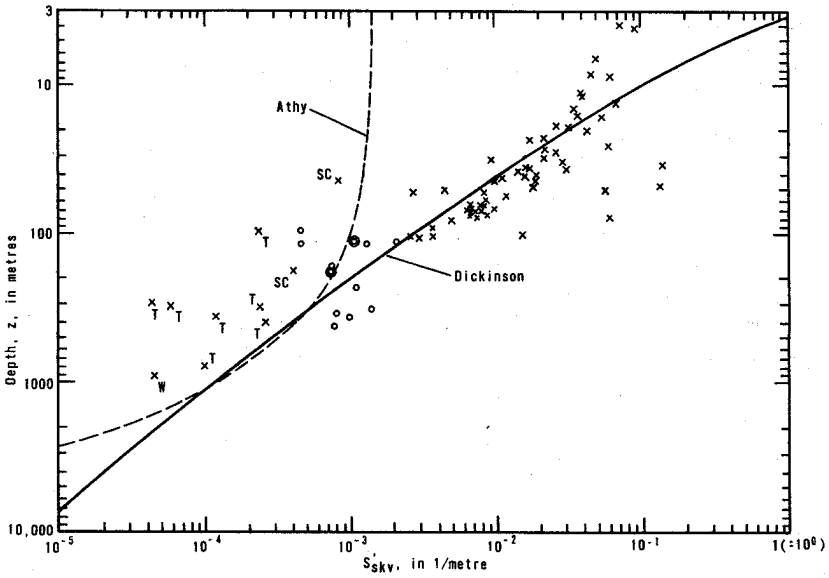

Figure 5.19 Specific storage for nonrecoverable compaction, S'_{skv}, as a function of depth, z.

Equation 5.44 tells us, as a first approximation, that for every foot of long-term drawdown, one can expect about one-tenth of a foot of ultimate compaction.

Let us interpret equation 5.44 in a somewhat broader time frame. One would expect a time lag of decades before compaction in the field would reach its ultimate value (equation 5.44) even under conditions of no recovery of artesian head. If at any time artesian head recovers above a transient critical elevation, ongoing residual subsidence will stop.

Predicting this critical elevation of head is discussed in the next section. Equation 5.44 and use of Dickinson's curve in Figure 5.19 tacitly requires sedimentary material within a con-

fined system initially to be normally consolidated. Another tacit assumption of equation 5.44 is that volume strain expresses itself entirely in vertical compression. For a confined aquifer system whose volume strain is isotropic, the vertical component of strain is one-third the volume strain. Whenever in situ strain is actually isotropic, use of Dickinson's curve (Figure 5.19) in equation 5.44 would thereby automatically give an estimate of vertical compression three times too large.

Methods for approximating a regional distribution of Δh_a, which appears in the left-hand side of equation 5.44, are available (e.g., Figueroa Vega, 1971). Discussion of these methods is beyond the scope of the present section.

5.3.6.2 Aquitard-drainage model

Tolman and Poland (1940) suggested that subsidence in the Santa Clara Valley, California, is caused not simply by declining artesian heads and the resulting compaction of permeable sands, but primarily by the nonrecoverable compaction of slow-draining clay layers within the confined system. This marks the conceptual birth of the aquitard-drainage model (Figure 5.20). Riley (1969) applied Terzaghi's (1925) theory of one-dimensional consolidation quantitatively to the aquitard-drainage model. Helm (1972, 1975, 1976) borrowed Riley's insights to develop a

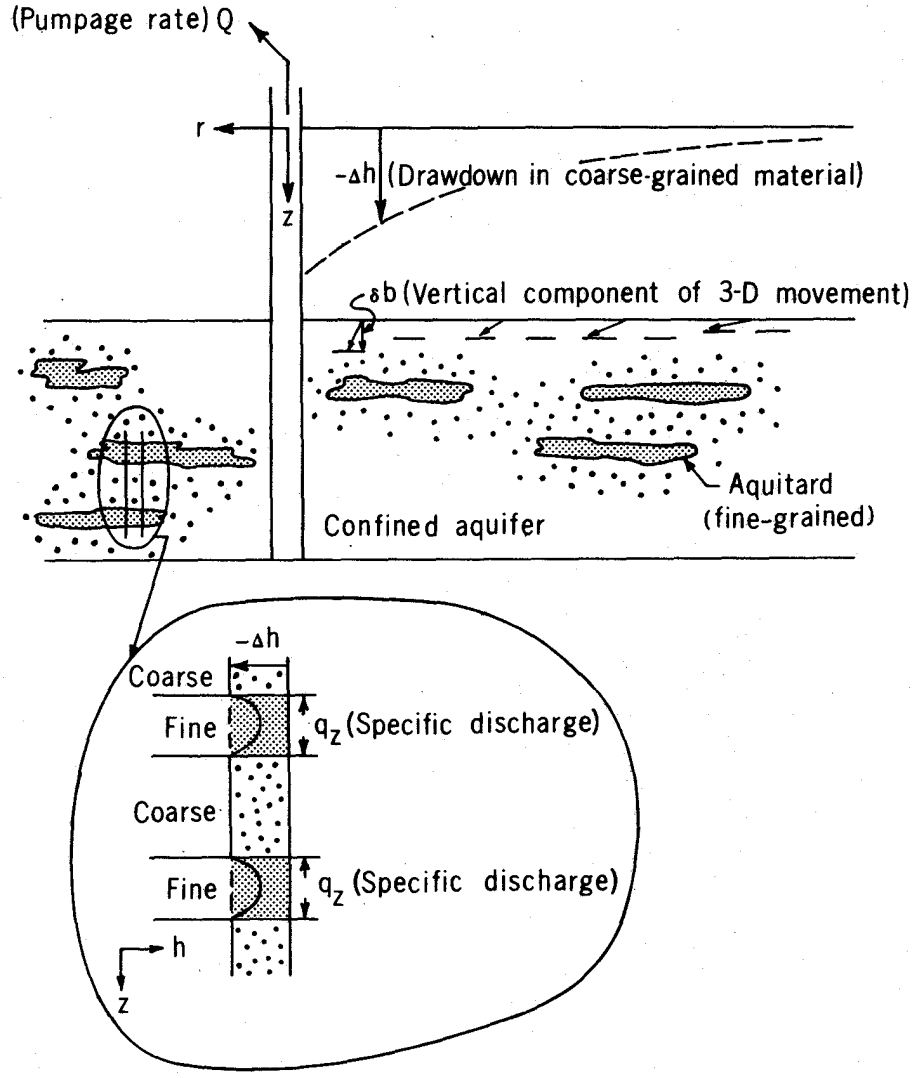

Figure 5.20 Aquitard-drainage model (modified from Helm, 1980, Figure 4).

one-dimensional computer code to simulate time-delayed aquitard compression and expansion in response to arbitrary fluctuations of hydraulic head within the coarse-grained portion of a confined aquifer system. In turn, Freeze (Witherspoon and Freeze, 1972; Gambolati and Freeze, 1973) and Narasimhan (Narasimhan and Witherspoon, 1977) borrowed Helm's insights for developing their own one-dimensional computer codes for aquifer-system compaction and expansion. Digitalizing the aquitard-drainage model led directly to a powerful predictive technique (Helm, 1978; Pollard and others, 1979) for land subsidence caused by water-level fluctuations within a confined aquifer system.

The aquitard-drainage model (Figure 5.20) represents the confined aquifer system as containing two basic types of porous material: a group of (i) fine-grained interbeds each of which is completely surrounded by a hydraulically connected system of (ii) coarse-grained material. The fine-grained interbeds (aquitards) are considered much less permeable than the interconnected coarse-grained portion of the confined aquifer system. Because slow-draining aquitards are interbedded within an aquifer, they are conceptually distinct from caprock, confining bed, or semi-confining bed that serves as a confined aquifer's upper boundary. The aquitard-drainage model conceptually attributes the observed time-lag (of compaction response to stress change) to the vertical component of fluid flow from one idealized material (aquitard) to another (aquifer) within the two-material system itself. The slow vertical drainage, q_z, from highly compressible aquitards to the less compressible aquifer material serves a somewhat similar rheological function in this model that a viscous "dashpot" serves in a viscoelastic reservoir model that has only one idealized undifferentiated material (Corapcioglu and Burtsaert, 1977).

In conjunction with appropriate field data, the model predicts (1) residual nonrecoverable compaction within a system, (2) time-dependent in situ preconsolidation pressure (a critical depth to water at which non-recoverable compaction is stopped during the unloading phase and is triggered during the reloading phase of a specified unloading-reloading cycle), and (3) a timeconstant, τ, for a confined system at a site of interest. According to Terzaghi's theory of consolidation, τ can be interpreted to represent the length of time required for initially unstressed aquitards to reach a 93 per-cent nonrecoverable compaction if water levels in adjacent aquifers (of a confined system) are instantaneously lowered a specified amount and then held constant.

By simulating field compaction and expansion at 8 sites in the Santa Clara Valley and 7 sites in the San Joaquin Valley, California, Helm (1978, Table 2) estimated that in 1978 residual compaction in the Santa Clara Valley ranged from a minimum of 0.52 m at one site to a maximum of 2.53 m at another. Among the analyzed sets of field data collected in the San Joaquin Valley, calculated residual compaction ranged from a minimum of 0.85 m at one site to a maximum of 9.75 m at another. In the early 1970's the critical depth to water was calculated site by site to range from a few to several tens of metres above a local past maximum depth to water. Time constants also were estimated from site-specific field data. In the Santa Clara Valley, τ was calculated to range from a minimum of 13 years at one site to 125 years at another. In the San Joaquin Valley τ was calculated to range from 5 years at one site to 1350 years at another.

Figures 5.21 and 5.22 illustrate the use of a one-dimensional computer simulation based on the aquitard-drainage model. Using the stress curve shown in the upper graph of Figure 5.21 as input values, parameter values within the mathematical model are calibrated in order to make calculated compaction (dotted line in the lower graph of Figure 5.21) be as close an approximation to observed compaction (solid line in the lower graph of Figure 5.21) as possible. Using these parameter values and the input stress curve shown in the upper graph of Figure 5.22, a predicted compaction curve is calculated for the period 1921-74. This prediction is shown by the solid line in the lower graph of Figure 5.22. Actual compaction is estimated as a portion of subsidence measured at bench mark J111 and is plotted as solid circles in the lower graph of Figure 5.22. The excellent agreement between predicted and observed compaction in Figure 5.22 confirms the parameter values found during the calibration process (Figure 5.21). This result increases one's confidence in the residual compaction, preconsolidation stress, and time constants that are estimated from this procedure.

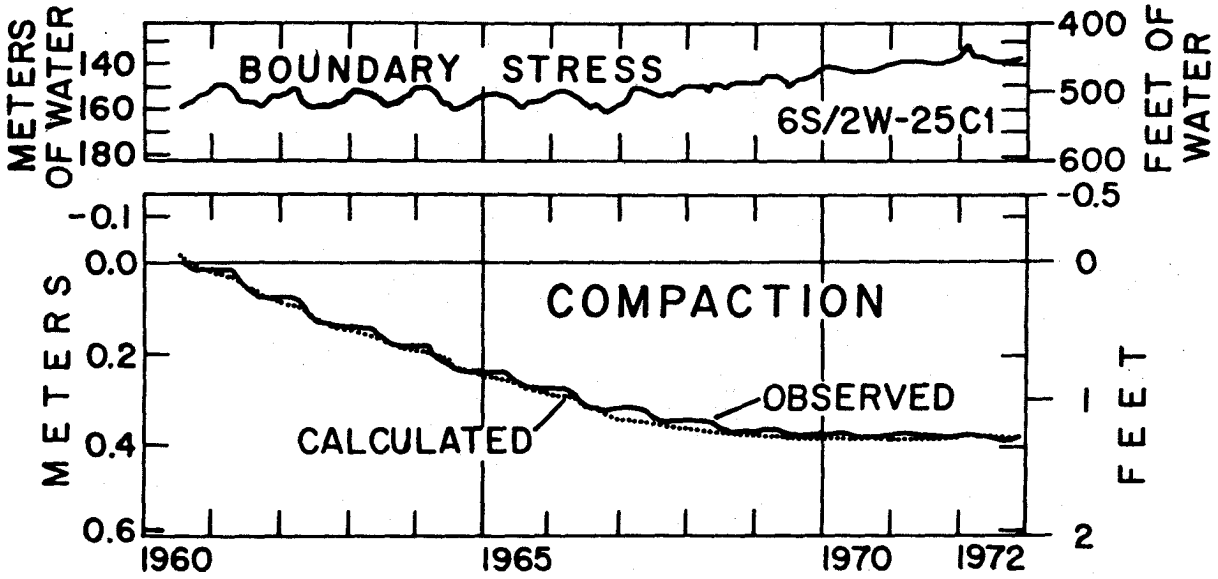

Figure 5.21 Simulation of compaction based on water-level data for well 6S/2W-25Cl (1960-72) and compaction data observed in well 24C3.

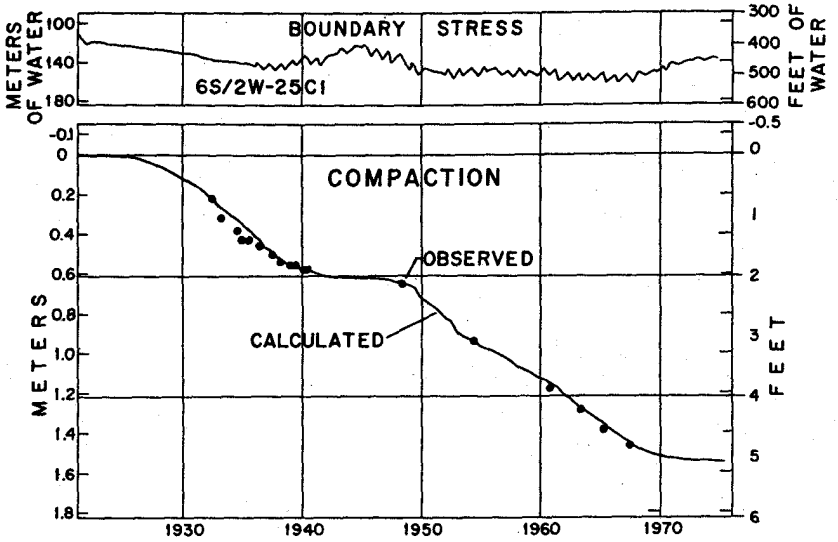

Figure 5.22 Simulation of compaction based on water-level data for well 6S/2W-25Cl (1921-74) and on compaction estimated as a portion of subsidence measured at bench mark

5.3.6.3 Influence of material within the unpumped overburden

Subsidence due to fluid withdrawal is the expression at land surface of the compression at depth of a stressed artesian aquifer system. Material within the intervening unpumped overburden may possibly play a role in mitigating land surface effects. Geertsma (1957, 1973) has in effect discussed quantitatively the role of the overburden. His equation for ultimate vertical displacement, U_z, directly over the center of an axially symmetric confined aquifer system (Figure 5.23) is

$$U_z(0, 0) = - 2((1-\nu)c_m b\Delta p \{1-[C/(1+C)^2]\}, \quad (5.45)$$

where

ν is Poisson's ratio,
b is thickness of compressing bed(s),
p is pressure change,
C is D/R,
D is depth to compressing bed(s), and
R is radius of stressed system.

For highly compressible poro-elastic bulk material, Geertsma's coefficient of uniaxial compaction, c_m, becomes

$$C_m = (1-2\nu)(1+\nu)/E(1-\nu), \tag{5.46}$$

where E is Young's modulus.

Equation 5.45 should be used with caution for the following reasons. Due to gravitational body forces on submerged solids, it is reasonable to assume that the base of a depressured aquifer system does not move upward. Unfortunately, Geertsma neglects such body forces in his analysis with the unrealistic result that under some circumstances the base of his idealized reservoir (confined aquifer system) mathematically moves upward a significant amount. This physically unlikely upward movement can mathematically nearly equal the total compaction of the stressed system. Hence there may mathematically be no downward movement of the top of the idealized reservoir. Correspondingly under these circumstances there would mathematically be no subsidence at land surface whatsoever. This questionable aspect of Geertsma's analysis reflects itself in equation 5.45.

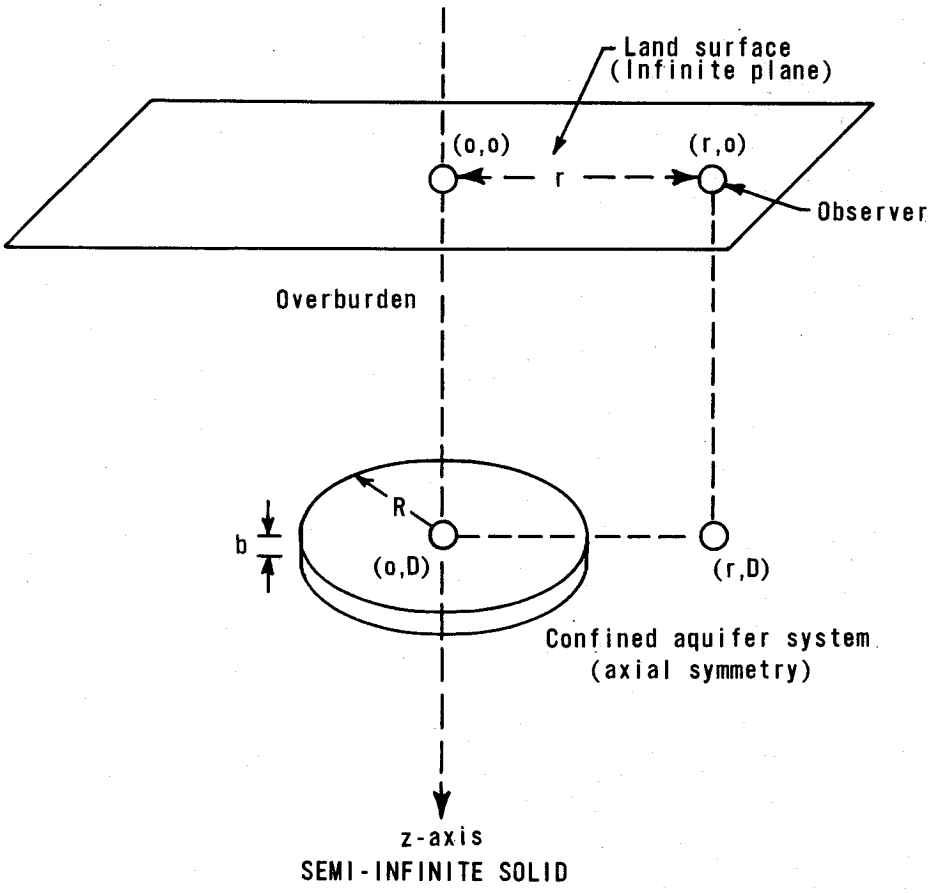

Figure 5.23 Half-space model (modified from Helm, 1980, Figure 2).

It is more reasonable to assume that the volume of compaction of a compressible aquifer system expresses itself eventually by an equal volume of subsidence at land surface. Whenever the upper boundary of a compacting aquifer system moves downward in response to compression of underlying sediments, Geertsma (1973) himself points out that the volume which this upper surface moves is preserved at land surface. When the vertical movement of the base of a confined aquifer system can realistically be considered negligible, land subsidence, according to Geertsma, equals volumetrically the total compaction of the confined aquifer system.

The areal distribution of subsidence is somewhat influenced, however, by the ratio of depth D to radius R (Figure 5.23) of the depressured confined aquifer system. The effect of compaction of an aquifer system with a large D/R ratio may be spread over a large area at land surface and hence minimize the vertical component of volumetric subsidence. The limit, however, would not be zero (which is erroneously implied by equation 5.45) but some finite fraction of b', of equation (5.44). For most ground-water systems the D/R ratio is sufficiently small that the overburden's spreading effect can be completely ignored. This implies the direct applicability of a depth-porosity model (Section 5.3.6.1).

The conceptual model used by many investigators, including Geertsma, will now be described. It is a variation of what can more generally be called a half-space model (Figure 5.23). The earth is represented as a homogeneous, isotropic, semi-infinite elastic (or poro-elastic) medium. Land surface is represented as a flat upper surface that is free to move. Neither calculated surface movement nor topographic relief affects the essential flatness of the idealized surface. Although a depressured zone at depth D below land surface with a center at radial distance r from an observer on land surface is represented by an idealized spherical tension center by Carrillo (1949), by vertical pincers by McCann and Wilts (1951), and by a radially symmetric group of strain nuclei by Geertsma (1957), the various representations are conceptually similar. Gambolati (1972) has discussed the major conceptual distinctions between the tension-center representation (Carrillo, 1949; McCann and Wilts, 1951) and the strain-nucleus representation (Mindlin and Cheng, 1950; Sen, 1950; Geertsma, 1957, 1966, 1973; Finol and Farouq Ali, 1975). Briefly, a tension center model tacitly requires an infinitely compressible reservoir within an elastic half-space. The strain-nucleus model requires the confined aquifer system's compressibility to equal the compressibility of the surrounding elastic halfspace. Finite heterogeneity between the compressing system and the surrounding half-space was introduced to the model by Gambolati (1972).

The question of finite heterogeneity deserves some comment. A confined aquifer system by definition yields fluid to a discharging well and experiences a pressure loss. The surrounding material by definition does not yield fluid. Hence porosity within a compressible confined aquifer system decreases. Porosity does not necessarily decrease within the surrounding halfspace. This distinction is analogous to the distinction in soil mechanics between drained and undrained compression. Decrease in porosity as a source for fluid discharge inherently introduces an extra component into a compressibility term for a confined aquifer system. This extra component does not appear in a corresponding compressibility term for the undrained surrounding half-space. Specifically, only S_{SW} of equation 3.3 is appropriate to use for the surrounding half-space whose individual grains are considered incompressible,, whereas the sum of S'_{SK} and S_{SW} is appropriate to use for the aquifer system itself. S'_{SK} is a function of porosity loss whereas S_{SW} is a function of the expansion of interstitial water. Hence, the hydraulics of underground fluid flow alone helps dictate the apparent heterogeneity of compressibilities between a compressing aquifer system and the surrounding half-space. This apparent or in situ hydraulic heterogeneity is distinct from standard differences in material properties which are tested and recorded in the laboratory.

5.4 REFERENCES

ALLEN, D. R., and MAYUGA, M. N. 1969. The mechanics of compaction and rebound, Wilmington oil field, Long Beach, California, USA, in Tison, L. J. (ed.), Land subsidence, Vol. 2. Internat. Assoc. Sci. Hydrology, Pub. 89, p. 4710-423.

ATHY, L. F. 1930. Density porosity, and compaction of sedimentary rocks. Bull. American Assoc. Petroleum Geologists, v. 14, p. 1-24.

BULL, W. B., and POLAND, J. F. 1975. Land subsidence due to ground-water withdrawal in the Los Banos-Kettleman City area, California, Part 3. Interrelations of water-level change, change in aquifer-system thickness, and subsidence. U. S. Geological Survey Professional Paper 437-G, 62 p.

CARRILLO, NABOR. 1949. Subsidence in the Long Beach-San Pedro area. Stanford Research Institute, p. 67-69.

CASTLE, R. 0., YERKES, R. F., and RILEY, F. S. 1969. A linear relationship between liquid production and oil-field subsidence, in Tison, L. J. (ed.), Land subsidence, Vol. 1. Internat. Assoc. Sci. Hydrology Pub. 88, p. 162-173.

CORAPCIOGLU, M. Y., and BRUTSAERT, W. 1977. Viscoelastic aquifer model applied to subsidence due to pumping. Water Resources Research, v. 13, p. 597-604.

DICKINSON, G. 1953. Geological aspects of abnormal reservoir pressures in Gulf Coast Louisiana. Bull. American Assoc. Petroleum Geologists, v. 37, no. 2, p. 410-432.

FIGUEROA VEGA, GERMÁN E. 1971. Influence chart for regional pumping effects. Water Resources Research, v. 7, no. 1, p. 209.

FIGUEROA VEGA, GERMÁN E. 1973. Aquifer and subsidence model for Mexico City. 85th Annual Meeting of The Geological Society of America, v. 5, no. 7, p. 620.

FIGUEROA VEGA, GERMÁN E. 1977. Subsidence of the City of Mexico; a historical review. Second Internat. Symposium on Land Subsidence Proc., IAHS-AISH Pub. 121, p. 35.

FINOL, A., and FAROUQ ALI, S. M. 1975. Numerical simulation of oil production with simultaneous ground subsidence. Jour. Soc. Petroleum Eng., p. 411-422.

GABRYSCH, R. K. 1969. Land surface subsidence in the Houston-Galveston region, Texas, in Tison, L. J., ed., Land subsidence, Vol. 1. Internat. Assoc. Sci. Hydrology, Pub. 88, p. 43-54.

GABRYSCH, R. K., and BONNET, C. W. 1976. Land-surface subsidence at Seabrook, Texas. U.S. Geological Survey Water-Resources Investigation 76-31, 53 p.

GAMBOLATI, G. 1972. A three dimensional model to compute land subsidence. Bull. Internat. Assoc. Hydrol. Sci., v. 17, no. 2, p. 219-226.

GAMBOLATI, G., and FREEZE, R. A. 1973. Mathematical simulation of the subsidence of Venice, 1, Theory. Water Resources Research, v. 9, no. 3, p. 721-733.

GEERTSMA, J. 1957. The effect of fluid pressure decline on volumetric changes of porous rocks. Trans. Amer. Soc. Mech. Engrs., AIME v. 210, p. 331-340.

GEERTSMA, J. 1966. Problems of rock mechanics in petroleum production engineering. Proc. First Cong. of the Internat. Soc. of Rock Mech., Lisbon, v. 1, p. 585-594.

GEERTSMA,J. 1973. A basic theory of subsidence due to reservoir compaction: the homogeneous case. Verhandeliger Kon. Ned. Geol. Mijhbouwk, v. 28, p. 43-62.

HELM, D. C. 1972. Simulation of aquitard compaction due to changes in stress [abs.]. EOS Trans. American Geophys. Union, v. 53, no. 11, p. 979.

HELM, D. C. 1975. One-dimensional simulation of aquifer system compaction near Pixley, Calif. 1, Constant parameters. Water Resources Research, v. 11, no. 3, p. 465-478.

HELM, D. C. 1976. One-dimensional simulation of aquifer system compaction near Pixley, Calif. 2, Stress-dependent parameters. Water Resources Research, v. 1, no. 3, p. 375-391.

HELM, D. C. 1978. Field verification of a one-dimensional mathematical model for transient compaction and expansion of a confined aquifer system, in Verification of mathematical and physical models in hydraulic engineering. Proc. 26th Hydraul. Div. Specialty Conf., College Park, Maryland, American Soc. Civil Eng., p. 189-196.

HERRERA, I., and FIGUEROA, G. E. 1969. A correspondence principle for the theory of leaky aquifers. Water Resources Research, v. 5, no. 4, p. 900-904.

HWANG, JUI-MING, and WU, CHIAU-MIN. 1969. Land subsidence problems in Taipei Basin, in Tison, L. J., ed., Land Subsidence, Vol. 1. Internat. Assoc. Sci. Hydrology, Pub. 88, p. 21-734.

IIDA, K. 1976. Land subsidence in Nobi Plain and change of water level. Rept. Commission on Environmental Protection, Nobi Area (Japan).

KUMAI, H., SAYAMA, M., SHIBASAKI, T., and UNO, K. 1969. Land subsidence in the Shiroishi Plain Kyushu, Japan, in Land Subsidence, Vol. 2. Internat. Assoc. Sci. Hydrology, Pub. 89, p. 645-657.

LOFGREN, B. E. 1969. Field measurement of aquifer-system compaction, San Joaquin Valley, California, USA, in Land Subsidence, Vol. 1. Internat. Assoc. Sci. Hydrology, Pub. 88, p. 272-284.

McCANN, G. D., and WILTS, C. H. 1951. A mathematical analysis of the subsidence in the Long Beach-San Pedro area. Calif. Inst. Technology, Tech. Rept., 117 p.

MAGARA, KINJI. 1978. Compaction and fluid migration. Elsevier Scientific Pub. Co., New York, 319 p.

MARSAL, R. J., and GRAUE, R. 1969. The subsoil of Lake Texcoco, in Carillo, Nabor, The subsidence of Mexico City and Texcoco Project. Secretaria de hacienda y credito publico fiduciarie, Mexico, p. 167-202.

MINDLIN, R. D., and CHENG, D. H. 1950. Thermoelastic stress in the semi-infinite solid. Jour. of Appl. Phys., v. 21, p. 931.

NARASIMHAN, T.N., and WITHERSPOON, P. A. 1977. Numerical model for land subsidence in shallow ground-water systems, Internat. Assoc. Sci. Hydrology Pub. 121, p. 133-144.

NEWMARK, N. M. 1942. Influence charts for computation of stresses in elastic foundations. University of Illinois, Bull. 40(12).

POLAND, J. F., LOFGREN, B. E., IRELAND, R. L., and PUGH, R. G. 1975. Land subsidence in the San Joaquin Valley, California, as of 1972. U.S. Geological Survey Professional Paper 437-H, 77 p.

POLLARD, W. S., HOLCOMBE, R. F., and MARSHALL, A. P. 1979. Subsidence cause and effect. Harris-Galveston Coastal Subsidence District Phase 1-A study, McClelland Engineers, Inc., Houston, Texas, 2 vols.

RILEY F. S. 1969. Analysis of borehole extensometer data from central California, in Tison, L. J., ed., Land subsidence, Vol. 2. Internat. Assoc. Sci. Hydrology, Pub. 89, p. 423-431.

SCHATZ, J. F., KASAMEYER, P. W. and CHENEY, J. A. 1978. A method of using in situ porosity measurements to place an upper bound on geothermal reservoir compaction, in Proc. Second Invit. Well Testing Symp., Berkeley, Calif. Lawrence Berkeley Laboratory.

SEN, B. 1950. Note on the stresses produced by nuclei of thermoelastic strain in a semi-infinite elastic solid. Quart. Appl. Math., v. 8, p. 635.

SHIBASAKI, T., KAMATA, A., and SHINTO, S. 1969. Hydrologic balance in the land subsidence phenomena, in Tison, L. J., ed., Land Subsidence, Vol. 2. Internat. Assoc. Sci. Hydrol. Pub. 88, p. 201-214.

TERZAGHI, KARL. 1923. Die Berechnung der Durchlassigkeitsziffer des Tones aus dem Verlauf der hydrodinamischen Spannungserscheinungen. Sitzber, Akad. Wiss. Wien, Abt. IIa, v. 132.

TERZAGHI, KARL. 1925. Settlement and consolidation of clay. Eng. News-Rec., McGraw-Hill, New York, p. 874-878, Nov. 26

THEIS, C. V. 1935. The relation between the lowering of piezometric surface and the rate and duration of discharge of a well using ground-water storage. Trans. American Geophys. Union, v. 16, p. 519-524.

TOLMAN, C. F., and POLAND, J. F. 1940. Ground-water, salt-water infiltration, and groundsurface recession in Santa Clara Valley, Santa Clara County, California. Trans., American Geophys. Union, pt. 1, p. 23-34.

WADACHI, K. 1940. Ground sinking in west Osaka (second rept.) Rept. Disaster Prevention Research Institute, No. 3.

WITHERSPOON, P. A., and FREEZE, R. A. 1972. The role of aquitards in a multiple-aquifer system. Penrose Conf. of the Geological Society of America, 1971, Geotimes, v. 17, no. 4, p. 22-24.

YAMAGUCHI, R. 1969. Water level change in the deep well of the University of Tokyo. Bull. Earthquake Research Institute, No. 47.